Depletion of antibiotic targets has widely varying effects on growth

Jun-Rong Wei[a], Vidhya Krishnamoorthy[a], Kenan Murphy[b], Jee-Hyun Kim[c], Dirk Schnappinger[c], Tom Alber[d], Christopher M. Sassetti[b,e], Kyu Y. Rhee[c,f], and Eric J. Rubin[a,1]

[a]Department of Immunology and Infectious Diseases, Harvard School of Public Health, Boston, MA 02115; [e]Howard Hughes Medical Institute, and [b]Department of Molecular Genetics and Microbiology, University of Massachusetts Medical School, Worcester, MA 01655; [c]Department of Microbiology and Immunology, Weill Cornell Medical College, New York, NY 10065; [d]Department of Molecular and Biology and QB3 Institute, University of California, Berkeley, CA 94720; [f]Department of Medicine, Weill Cornell Medical College, New York, NY 10065

Edited* by John J. Mekalanos, Harvard Medical School, Boston, MA, and approved February 1, 2011 (received for review December 7, 2010)

It is often assumed that antibiotics act on the most vulnerable cellular targets, particularly those that require limited inhibition to block growth. To evaluate this assumption, we developed a genetic method that can inducibly deplete targeted proteins and that mimics their chemical inactivation. We applied this system to current antibiotic targets in mycobacteria. Although depleting some antibiotic targets significantly perturbs bacterial growth, surprisingly, we found that reducing the levels of other targets by more than 97% had little or no effect on growth. For one of these targets, dihydrofolate reductase, metabolic analysis suggested that depletion mimics the use of subinhibitory concentrations of the antibiotic trimethroprim. These observations indicate that some drug targets can exist at levels much higher than are needed to support growth. However, protein depletion can be used to identify promising drug targets that are particularly vulnerable to inhibition.

inducible proteolysis | HIV protease | trimethoprim

The rise of drug resistance has prompted a renewed search for antibacterial compounds (1). Although bacteria have many essential processes that could serve as targets for antibiotics, most current drugs act on a limited number of targets in just a handful of pathways (2). To define pathways that could serve as drug targets, we must first understand the properties that make existing drug/target pairs so effective. Several properties contribute to the efficacy of antibiotics (3). These include the importance of the target in normal cell physiology, the degree of inhibition required to block cell growth or induce cell death, and chemical properties, including potency (the concentration of compound required to inhibit growth) and off-target effects. Although there are many potential targets in bacteria, target-based strategies to develop antibiotics have been disappointing (2).

Tuberculosis remains a major public health problem, and antibiotic development is being actively pursued (4, 5). Using transposon mutagenesis and DNA microarray analysis, we have identified genes that are essential for the growth of *Mycobacterium tuberculosis*, the causative organism of tuberculosis (6). However, not all of these represent equivalently attractive antibiotic targets. One characteristic that determines the susceptibility of a target is how much inhibition is required to block cell growth, a property that we define as vulnerability. Inhibitors that have equivalent potency against the isolated target will be far more effective against highly vulnerable targets (7). Thus, if we are able to evaluate vulnerability, we can rationally prioritize among a long list of potential targets for antibiotic development.

To examine the vulnerability of current antibiotic targets, we designed a genetic method that can inducibly deplete target proteins in response to the addition of a single small molecule. This method allows us to specifically assess the vulnerability of current drug targets. Our approach is based on controlling protein levels instead of more traditional approaches that modulate gene transcription or mRNA stability. Using inducible protein degradation rather than regulating mRNA levels allows us to study long-lived proteins and maintain native expression levels.

Results and Discussion

Inducible Protein Degradation System. To regulate protein degradation, we used the Clp protease system that is widely conserved among bacteria. Clp consists of the highly processive ClpP protease and several accessory proteins that identify targets and help denature them before proteolysis (8). Although these factors can recognize a number of different amino acid sequences, the best characterized is SsrA, a short peptide that is added to the C terminus of incomplete proteins at stalled ribosomes (9). In *Escherichia coli*, SsrA-tagged proteins are recognized by two accessory factors, ClpX and SspB, and are delivered to ClpP for rapid degradation (10). Our strategy relies on appending a modified SsrA tag, masking the sequence to the target protein of interest, and inducing degradation by revealing the SsrA sequence at the C terminus using HIV-2 protease (Fig. 1*A*).

Although Clp and its accessory factors have been conditionally expressed in other bacteria (11, 12), the two subunits of the Clp protease and many associated factors seem to be required for normal growth in mycobacteria (6), suggesting that altering their expression level might have unwanted physiological effects. Instead, we chose to modify the target protein and use the endogenous protease. We initially confirmed that the SsrA sequence must be located at the C terminus of a protein to mediate degradation; the addition of more amino acids results in completely stable proteins (Fig. S1). Based on this observation, we developed an inducible degradation (ID) system. We engineered a C-terminal peptide, the ID tag (Fig. 1 *A* and *B*), consisting of the mycobacterial SsrA sequence (with the substitution of a single amino acid) fused to a downstream protecting peptide, which can be cleaved by a site-specific protease derived from an HIV-2 isolate. Induction of HIV-2 protease expression exposes the C terminus of the SsrA sequence and targets the protein for Clp-mediated proteolysis. We incorporated a FLAG tag (DYKDDDDK) at the C terminus of the ID tag to track uncleaved target protein and a c-myc tag (EQKLISEEDL) at the N terminus to monitor the stability of protein after cleavage.

Expression of GFP fused to the ID tag in *M. smegmatis* yielded fluorescent cells in the absence of HIV-2 protease (Fig. S1). In

Author contributions: J.-R.W. and E.J.R. designed research; J.-R.W. and V.K. performed research; K.M., J.-H.K., D.S., T.A., C.M.S., and K.Y.R. contributed new reagents/analytic tools; J.-R.W., C.M.S., K.Y.R., and E.J.R. analyzed data; and J.-R.W., J.-H.K., D.S., T.A., C.M.S., K.Y.R., and E.J.R. wrote the paper.

The authors declare no conflict of interest.

*This Direct Submission article had a prearranged editor.

Data deposition: The sequences reported in this paper have been deposited in the GenBank database (accession nos. GU459073–GU459081).

[1]To whom correspondence should be addressed. E-mail: erubin@hsph.harvard.edu.

This article contains supporting information online at www.pnas.org/lookup/suppl/doi:10.1073/pnas.1018301108/-/DCSupplemental.

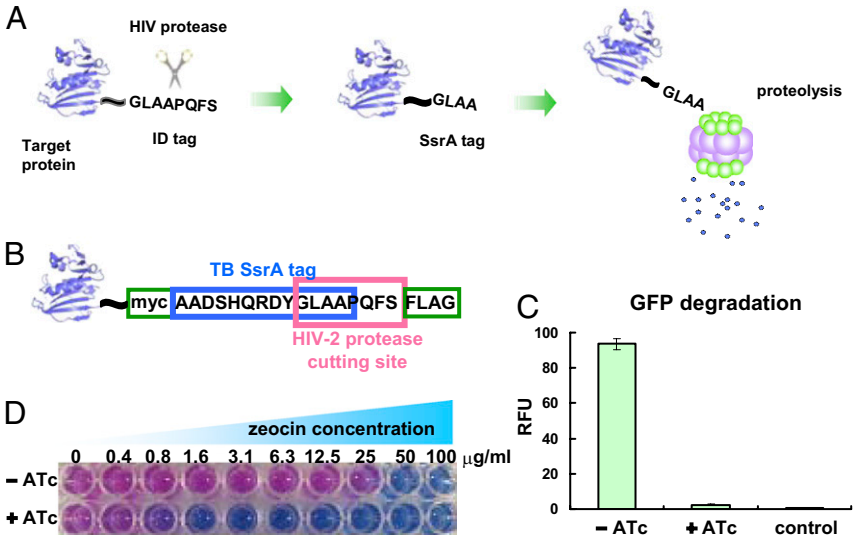

Fig. 1. The inducible degradation (ID) tag. (*A*) ID-tagged proteins are stable in the absence of HIV-2 protease but are degraded after proteolytic removal of the protecting peptide. (*B*) The ID tag is composed of two parts, a mutated mycobacterial SsrA sequence and a protecting peptide, separated by an HIV-2 protease recognition site. A c-myc epitope at the N terminus and a FLAG epitope at the C terminus of the ID tag permit immunodetection of target proteins. (*C*) Fluorescence of GFP fused to the ID tag in *M. smegmatis* carrying an inducible HIV-2 protease. Fluorescence is lost on overnight induction of HIV-2 protease using anhydrotetracycline (ATc). (*D*) The Zeocin resistance (Zeo) protein is efficiently degraded by the ID tag. *M. smegmatis* mc^2155 containing both pGH1000A::zeo-ID and pMC1s::WT-HIV2Pr was grown in 96-well plates with varying concentrations of Zeocin or ATc. Expression of HIV-2 protease decreases the observed MIC (the concentration of antibiotic necessary to block conversion to a pink color).

the absence of the inducer, anhydrotetracycline (ATc) (13), the presence of a plasmid encoding a tetracycline-inducible HIV-2 protease gene (codon-optimized for expression in mycobacteria) had no effect on fluorescence (Fig. S1). With added ATc, fluorescence intensity dropped to baseline after overnight incubation (Fig. 1*C*). Similarly, when we fused the ID tag to the Zeocin resistance protein (which mediates resistance to this bleomycin family drug by binding and neutralization) (14), we found that the Zeocin minimal inhibitory concentration (MIC) was identical in a strain that lacked HIV-2 protease and a strain containing inducible HIV-2 protease in the absence of ATc (Fig. S2). The addition of inducer resulted in dramatic target depletion, and bacteria were sensitized to Zeocin by approximately 32-fold (Fig. 1*D*).

Antibiotic Targets Can Be Tagged and Inducibly Degraded. The ID tag system allowed us to test the common view that antibiotics act largely by reducing the target activity below a threshold level. We chose six antibiotic target proteins: RNA polymerase β-subunit (RpoB), the target of rifampicin; gyrase A subunit (GyrA), the target of quinolones (15); alanine racemase (Alr), the target of D-cycloserine (16); dihydrofolate reductase (DHFR), the target of trimethoprim; enoyl reductase InhA, the target of isoniazid (17), and β-ketoacyl-acyl-carrier protein synthase KasA, the target of thiolactomycin (18). We used phage-mediated homologous recombination (recombineering) (19) to insert the ID tag into *M. smegmatis* chromosomal genes to make these diverse antibiotic targets of ID tag fusion protein. In each ID-tagged strain, we separately integrated a copy of the HIV-2 protease gene regulated by a tetracycline-dependent promoter. Without induction, these target proteins are expressed by their native promoter to execute their function, and after induction, the cleavage by HIV-2 protease will mark these proteins for degradation.

All six antibiotic targets were significantly depleted on induction of HIV-2 protease (Fig. 2*A*). Quantitative Western blotting revealed that incubation with inducer depleted the targets to different extents. Although RpoB levels remained at ~20% of the levels observed without inducer, >97% of the ID-tagged Alr was degraded (Fig. 2*B*). Degradation of InhA, Alr, and DHFR was essentially complete within 3 h (Fig. 2*C*), whereas there was little depletion of RpoB or GyrA at 6 h (Fig. S3). The proteins that were less rapidly depleted could be more resistant to proteolysis or could be up-regulated in response to depletion, which might be the case for KasA (20).

Growth Defects Do Not Necessarily Correlate with the Degree of Protein Depletion. If killing were proportional to the reduction in target enzyme activity mediated by these antibiotics, we expected that bacterial growth and survival would correlate with the degree of protein depletion. We measured the growth rate of each strain in the presence or absence of inducer beginning either directly (for rapidly depleted proteins) or 12 h (for slowly depleted proteins) after addition of inducer. However, we found very little correlation between protein abundance and growth. Efficient InhA depletion resulted in bacterial death, whereas >97% depletion of DHFR and Alr only modestly slowed growth. However, modest depletion of RpoB led to a dramatic growth arrest (Fig. 3).

To confirm that the ID tag mediated selective degradation (and not just, for example, removal of the tag), we used two different approaches that showed that target proteins were functionally inactivated. First, HIV-2 protease induction caused hypersensitivity to antibiotics targeting the depleted protein but not to other antibiotics (Fig. 4*A*). These results show that ID tag-mediated proteolysis results in functional depletion of each target and confirm that they are the targets for the cognate antibiotics. Second, we directly assayed enzyme activity for two targets, DHFR and Alr. In both cases, we found markedly reduced activity consistent with the results of immunoblotting (Fig. 4*B*). Thus, cells grew rapidly, despite marked depletion of these critical proteins.

Depletion of Dihydrofolate Reductase Resembles the Use of Subinhibitory Antibiotic Concentrations. Depletion of DHFR fails to phenocopy treatment with trimethoprim, a presumed inhibitor of the enzyme. This could be caused by at least three different

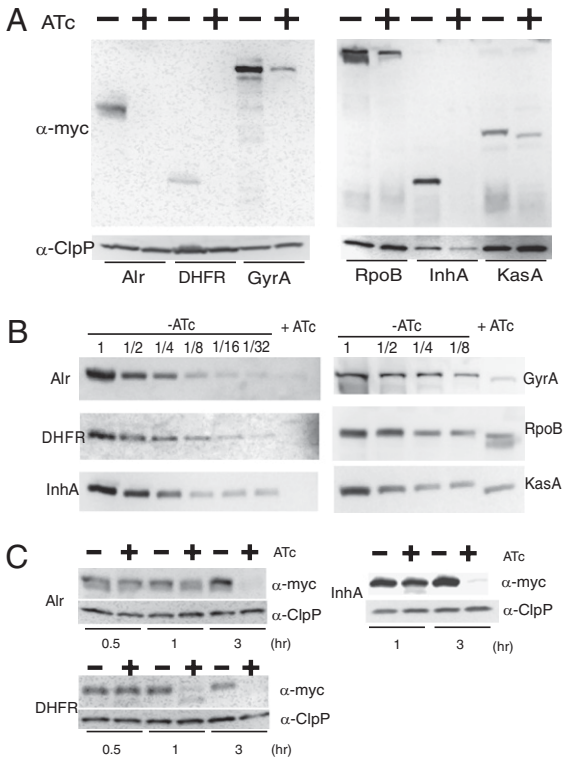

Fig. 2. Degradation of endogenous proteins fused to the ID tag. Western blot analysis of lysates carrying ID tag fusions to target proteins in the presence or absence of inducer (ATc) was performed using α-c-myc antibody to visualize ID-tagged proteins or α-ClpP antibody as a loading control. (*A*) Samples were collected 15 h after the addition of inducer. Loading of each lane was normalized using culture OD. (*B*) Semiquantitative Western blot of serially diluted lysates from strains grown in the absence of inducer compared with induced lysates (far right lane). (*C*) Time course of degradation. Lysates were collected at the indicated time points and normalized by culture OD.

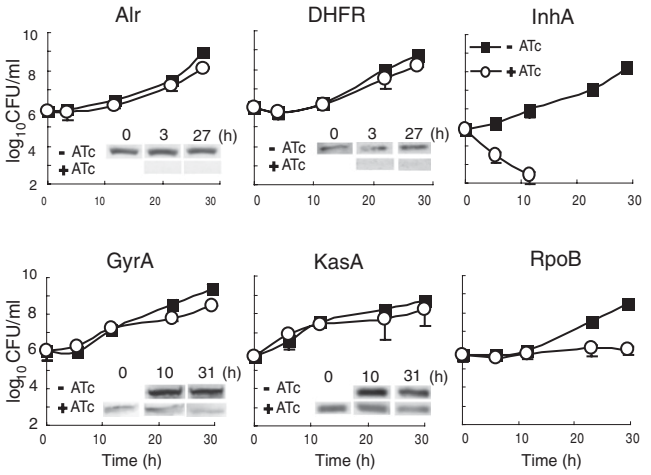

Fig. 3. Growth of strains after protein depletion. Strains carrying ID tags fused to GyrA, KasA, and RpoB were grown to midlog phase and preincubated with ATc for 12 h to allow protein degradation to proceed. Strains harboring ID tag fusions to Alr, DFHR, and InhA were not preincubated. To measure growth, strains were diluted 1:100 into fresh medium with or without ATc, and samples were removed at indicated time points for cfu determination. *Insets* show the amount of remaining protein at indicated time points as determined by Western blotting using anti–c-myc antiserum. A strain carrying the HIV-2 protease gene but no ID tag grew normally in the presence of ATc (Fig. S4).

mechanisms. Trimethoprim could have multiple targets along with DHFR, and inhibition could require those additional activities. The drug might not be a simple inhibitor and may alter enzyme activity in a manner that induces toxicity (15, 21, 22) or activates a cell death pathway (23–25). Finally, trimethoprim might simply produce a greater degree of inhibition than is seen with target depletion.

To distinguish these possibilities, we used metabolic profiling. We expected one of two patterns. If trimethoprim had additional targets or induced complex alterations in enzyme activity, we should see different changes in metabolites than those changes induced by target depletion. However, to see these effects, we needed to treat with subinhibitory concentrations of trimethoprim to avoid seeing secondary changes in metabolites associated with altered growth rate.

To perform the metabolic assays, we grew bacteria on filters to allow rapid lysis. Under these conditions, we found that depletion of DHFR was still induced by low concentrations of ATc (Fig. S5*A*). As seen in broth cultures, filter-grown cells exhibited only modest growth defects after DHFR depletion (Fig. S5*B*). We found that somewhat higher concentrations of trimethoprim were required to inhibit growth on filters than in broth. However, as in broth culture, bacteria became hypersusceptible to trimethoprim after DHFR depletion (Fig. S5*B*).

We examined the concentrations of a large set of identified and unidentified metabolites after DHFR depletion or treatment with trimethoprim. In agreement with previous results (26), we saw a number of metabolites whose concentration changed markedly and that are consistent with the known biochemical pathway. Homocysteine, deoxyuridine monophosphate (dUMP), serine, and aminoimidazole carboxamide ribonucleotide (AICAR) increased dramatically with either DHFR depletion or trimethoprim treatment (Fig. S5*C*). Higher concentrations of trimethoprim evoked considerably larger changes in the same metabolites as well as additional alterations.

We reasoned that, if DHFR is the main target of trimethoprim, than the metabolic changes induced by drug treatment should be mimicked by DHFR depletion. In addition, treatment with drug after DHFR depletion should show similar metabolic effects but at lower trimethoprim concentrations. To test this prediction, we compared the metabolic profile induced by various concentrations of trimethoprim with or without DHFR depletion. We saw changes in the concentration-dependent effects of several metabolites. In all cases, metabolic changes after DHFR depletion were similar to bacteria with WT levels of DHFR treated with subinhibitory concentrations of trimethoprim. In bacteria depleted of DHFR, trimethoprim induced changes similar to those seen in WT cells but at lower drug concentrations (representative metabolites are shown in Fig. 5*B*). Therefore, it seems that trimethoprim acts primarily as a DHFR inhibitor.

Inducible Protein Degradation Helps to Classify Drug Targets by Their Sensitivity to Depletion. In our study, we found that depletion of drug targets results in varying effects. The cidal effects of reducing the level of InhA protein seen, albeit more slowly, with an inducible promoter substitution (17) suggest that, although isoniazid may target multiple enzymes (27–29), inhibition of InhA alone could account for antibiotic activity. The rapid cell death seen with InhA depletion and the growth cessation with even only mild depletion of RpoB suggest that these biochemical processes are hypersensitive to inhibition. In contrast, targets like DHFR and alanine racemase are present in considerable excess. Thus, drugs that target these enzymes have special properties. Trimethoprim, for example, induces high levels of

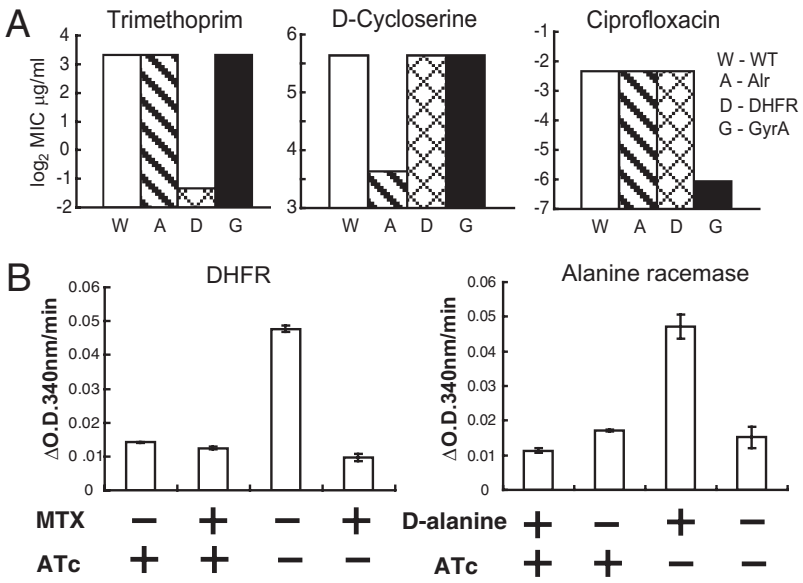

Fig. 4. MIC to antibiotics and enzymatic activities in protein-depleted strains. (*A*) Antibiotic susceptibilities of strains after protein depletion. White (WT), hatched (Alr), cross-hatched (DHFR), and black (GyrA) bars represent $\log_2$ MIC values after depletion of designated proteins. (*B*) Strains carrying ID tag fusions to DHFR (*Left*) and Alr (*Right*) were assayed for enzymatic activity after overnight culture with and without targeted degradation. Because we used crude lysates, background for the DHFR assay was determined in the presence of saturating DHFR inhibitor, methotrexate (MTX; 1 μM). Background for the alanine racemase assay was determined by omitting the substrate, D-alanine.

inhibition, either because the compound is particularly potent or it achieves high local concentrations at its target.

Although many proteins are essential for bacterial growth and survival, these potential antibiotic targets vary widely in how much inhibition is required to block cellular replication or induce death. This is true even for the targets of known drugs. Proteins such as InhA or RpoB, whose activity needs only limited inhibition to block bacterial growth, are particularly attractive as targets for new drugs. In other cases, the target/compound pair has unique properties. For example, fluoroquinolone antibiotics not only inhibit DNA gyrase but also prevent religation of cleaved DNA, leading to double-stranded breaks (30). Similarly,

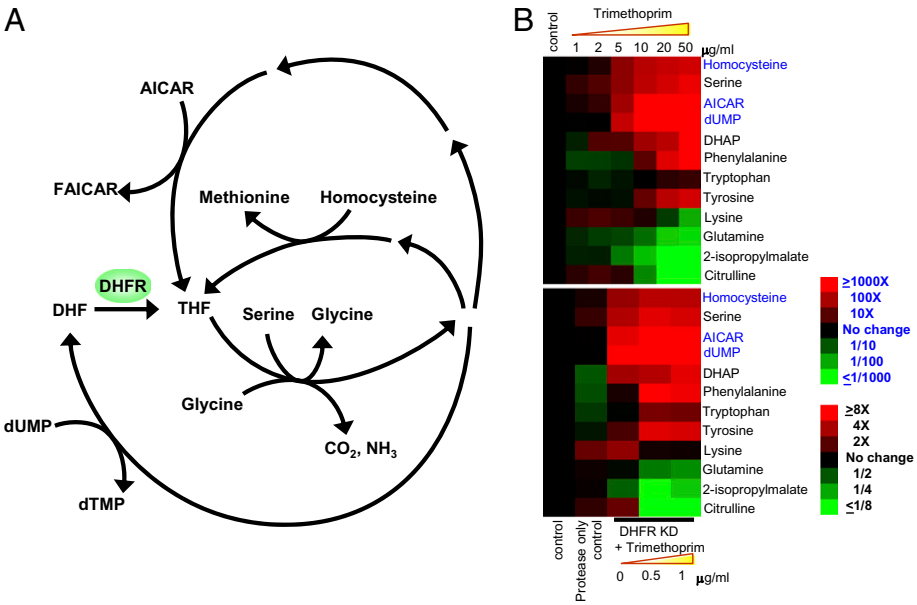

Fig. 5. Metabolites affected by DHFR depletion or trimethoprim treatment. (*A*) Biochemical pathways related to DHFR. (*B*) Profiles of 12 intracellular metabolites in *M. smegmatics* treated with trimethoprim or depleted of DHFR. Relative levels are expressed as the log ratio of signal intensity normalized to the control sample, which was untreated cells. For dUMP, AICAR, and homocysteine, the numbers are in $\log_{10}$, and for the rest metabolites, the numbers are in $\log_2$. Both drug treatment and DHFR depletion were performed on the same strain, which has an ID-tagged DHFR and inducible protease on the chromosome. Protease-only control cells were induced for protease but not depleted for DHFR. Trimethoprim cells (*B Upper*) were treated with various concentrations of trimethoprim but not depleted for DHFR. DHFR-KD + trimethoprim (*B Lower*) indicates bacteria grown in the presence of various concentrations of trimethoprim and ATc 50 ng/mL, which depletes DHFR to less than 2% of its physiological concentration. This experiment was performed in duplicate, and this result is representative of three independent experiments. Metabolite signal intensities were normalized to total protein in the lysates.

antibiotics that affect protein synthesis can kill cells by blocking protein secretion (22). Such unique interactions can be critical for drug action but cannot easily be modeled in mutant bacterial strains. However, the genetic strategy described here is a useful approach to identifying targets that could be very effective targets for compounds that are pure inhibitors.

Methods

Bacterial Strains and Culture Conditions. *M. smegmatis* strains were grown at 37 °C with shaking in Middlebrook 7H9 (Difco) supplemented with 0.2% glycerol, 0.05% Tween-80, 0.5% BSA, 0.2% dextrose, and 0.085% sodium chloride. Mycobacterial transformation was done as described (31), and transformants were grown on LB agar (Difco).

The final concentrations of antibiotics used for *E. coli* were 100 μg/mL for ampicillin, 150 μg/mL for hygromycin, and 50 μg/mL for kanamycin. For *M. smegmatis*, concentrations were 50 μg/mL for hygromycin and 20 μg/mL for kanamycin. ATc was added to cultures at a final concentration of 50 ng/mL unless otherwise stated.

Antibodies, Plasmids, and Primers. The plasmids and primers used in this study are listed in Tables S1–S3.

Pfu Polymerase (Stratagene) or Phusion polymerase (New England Biolabs) was used for all PCR. Primers (Invitrogen), restriction enzymes (New England Biolabs), sequencing (GENEWIZ), synthetic genes (GenScript), anti–c-myc antibody (used as 1:10,000 dilution; Novus), and reagents for Western blots (ThermoScientific) were obtained from commercial sources. Anti-ClpP antibody was a gift from Olga Kandror and Alfred Goldberg.

Inserting ID Tag into Substrate Gene by Phage-Mediated Recombineering. Substrates were designed to have at least 120 bp chromosomal homology in each flank. For GyrA and RpoB, long primer pairs (gyrA-mycF1, gyrA-mycF2, gyrA-hygR1, gyrA-hygR2, rpoB-mycF1, rpoB-mycF2, rpoB-hygR1, and rpoB-hygR2) were used to generate substrate PCR products using two rounds of PCR from template plasmid pBSK::zeo-ID-hyg. For Alr, DHFR, InhA, and KasA, primer pairs (dfrAF, dfrAR, alrF, alrR, inhAF, inhAR, kasAF, and kasAR) were used to generate substrate PCR products from template plasmids pUC57::alr-ID-hyg, pUC57::dfrA-ID-hyg, pUC57::inhA-ID-hyg, and pUC57::kasA-ID-hyg, respectively.

To prepare competent cells for recombineering, a stationary culture of *M. smegmatis* with pNit::ET (GenBank no. GU459073) was diluted to 1:100, and the inducer isovaleronitrile was added to a final concentration of 10 μM. The culture was grown overnight to OD_{600} = 0.8–1.0, and competent cells were prepared (31). Electroporation was performed as previously described (31). Positive clones (by Western blot) were plated on LB agar containing 10% sucrose to counterselect against the recombinase plasmid and then, were scored for growth on kanamycin-containing medium to confirm the loss of pNit::ET.

Fluorescence Measurement. Bacterial strains were grown to stationary phase and then back-diluted to 1:100 in fresh medium; 150 μL culture were taken, and fluorescence was measured at 485/520 nm by Fluoroskan ascent FL (ThermoScientific). Results represent the median ± SD of triplicate samples.

Zeocin Susceptibility Assay by Alamar Blue. We used a modification of the method described by Franzblau et al. (32). Briefly, Zeocin was serially diluted into Middlebrook 7H9 broth. Bacterial cultures were grown to midlog phase (OD_{600nm} = 0.5) and diluted to a calculated OD_{600} = 0.001; 90 μL culture were added to each well. The leftmost column of the 96-well plate contained no antibiotic. Plates were sealed with breathable film (VWR) and incubated at 37 °C for 24 h. Alamar Blue (Biosource) reagent was added to each well, and plates were reincubated for an additional 12 h at 37 °C. The MIC was defined as the lowest drug concentration that prevented a color change from blue to pink.

Western Blot Analysis. Total protein lysates were prepared from equivalent cell numbers using bead beating, and Western blot analysis was performed as previously described (33). For Fig. 2, bacterial cultures were grown to stationary phase, diluted 1:20 with fresh medium with or without ATc, and then cultured for 12–15 h. For Fig. 3, cultures for Western blots were grown in parallel to those used for cfu determination as described in Fig. 3. Detection was performed using SuperSignal West Femto Chemiluminescent Substrate (ThermoScientific) according the manufacturer's protocol. In all cases, blots were stripped and reprobed with anti-ClpP to ensure equivalent loading of samples.

Growth Curve of Viability. Strains were grown at 37 °C up to log phase (OD_{600} ~ 0.4). Cultures were diluted 1:100 into fresh medium with or without ATc. Strains with knockdowns of GyrA, KasA, and RpoB were preincubated with ATc for 12 h; the remainders were not preincubated. cfu was determined by plating and colony counting. Results represent mean ± SD for triplicate samples.

Enzyme Activity Assay of DHFR and Alanine Racemase. Bacterial cultures were grown to stationary phase, diluted 1:50 to fresh medium with or without ATc, and cultured for 12–15 h. On harvest, cell numbers were normalized using OD_{600} determination. Cells were centrifuged and washed with 1 mL 1× DHFR assay (for DHFR) buffer or 100 mM Tricine/NaOH (pH 8.5; for alanine racemase assay), and then, they were resuspended in 300 μL same buffer. Cells were lysed by bead beating three times for 45 s. Protein concentrations were measured using the Bradford assay (Quick Start; Bio-Rad) to normalize the amount for enzyme activity assay. DHFR assay was performed using the Dihydrofolate Reductase Assay Kit (Sigma) according the manufacturer's protocol. Alanine racemase activity was measured spectrophotometrically at room temperature as described previously (34). Results represent mean ± SD for triplicate samples.

Metabolomic Analysis. Bacterial cultures were first grown to OD = 1.0 and then inoculated onto 0.22-μm nitrocellulose filters under vacuum filtration. Filters with bacteria were then placed atop 7H10 agar with supplements and suitable supplements, such as ATc (50 ng/mL) or varying concentrations of trimethoprim, and allowed to grow at 37 °C. We determined cfu by scraping bacteria from the filter 24 h after inoculation followed by resuspension in 7H9 medium before quantitative culture. To determine metabolite concentrations, we first sequenced by plunging filters into acetonitrile/methanol/H_2O (40:40:20) precooled to −40 °C and then disrupted cells using bead beating with 0.1 mm Zirconia beads in a Precellys tissue homogenizer. Lysates were clarified by centrifugation and then filtered across a 0.22-mm filter. To normalize bacterial biomass of individual samples, we determined the residual protein content of metabolite extracts by Bradford assay. Liquid chromatography-MS for lysates was performed as previously described (35).

ACKNOWLEDGMENTS. We thank H. Eoh and P. Kim for technical help with the metabolic assay; J. Mekalanos, S. Fortune, B. Javid, M. Chao, W.-L. Lo, M. Fernandez-Suarez, C. Maher, and C. Craik for helpful discussions; and P. Kanki and N. Ulenga for providing the HIV-2 DNA clone. This work was supported by the Taiwan Merit Scholarship (to J.-R.W.), the Heiser Grant of the New York Community Trust (to J.-R.W.), grants from the Bill and Melinda Gates Foundation (to D.S., C.M.S., and E.J.R.), Bill and Melinda Gates Foundation TB Drug Accelerator Program Grant 42848 (to D.S.), and National Institutes of Health to the TB Structural Genomics Consortium Grants P01AI68135 (to T.A.) and R01AI071881 (to E.J.R.).

1. Fischbach MA, Walsh CT (2009) Antibiotics for emerging pathogens. *Science* 325: 1089–1093.
2. Payne DJ, Gwynn MN, Holmes DJ, Pompliano DL (2007) Drugs for bad bugs: Confronting the challenges of antibacterial discovery. *Nat Rev Drug Discov* 6:29–40.
3. Kohanski MA, Dwyer DJ, Collins JJ (2010) How antibiotics kill bacteria: From targets to networks. *Nat Rev Microbiol* 8:423–435.
4. Sacchettini JC, Rubin EJ, Freundlich JS (2008) Drugs versus bugs: In pursuit of the persistent predator *Mycobacterium tuberculosis*. *Nat Rev Microbiol* 6:41–52.
5. Balganesh TS, Alzari PM, Cole ST (2008) Rising standards for tuberculosis drug development. *Trends Pharmacol Sci* 29:576–581.
6. Sassetti CM, Boyd DH, Rubin EJ (2003) Genes required for mycobacterial growth defined by high density mutagenesis. *Mol Microbiol* 48:77–84.
7. Barry CE, 3rd, et al. (2009) The spectrum of latent tuberculosis: Rethinking the biology and intervention strategies. *Nat Rev Microbiol* 7:845–855.
8. Moore SD, Sauer RT (2007) The tmRNA system for translational surveillance and ribosome rescue. *Annu Rev Biochem* 76:101–124.
9. Keiler KC, Waller PR, Sauer RT (1996) Role of a peptide tagging system in degradation of proteins synthesized from damaged messenger RNA. *Science* 271: 990–993.
10. Levchenko I, Seidel M, Sauer RT, Baker TA (2000) A specificity-enhancing factor for the ClpXP degradation machine. *Science* 289:2354–2356.
11. McGinness KE, Baker TA, Sauer RT (2006) Engineering controllable protein degradation. *Mol Cell* 22:701–707.
12. Grilly C, Stricker J, Pang WL, Bennett MR, Hasty J (2007) A synthetic gene network for tuning protein degradation in *Saccharomyces cerevisiae*. *Mol Syst Biol* 3:127.
13. Ehrt S, et al. (2005) Controlling gene expression in mycobacteria with anhydrotetracycline and Tet repressor. *Nucleic Acids Res* 33:e21.

14. Drocourt D, Calmels T, Reynes JP, Baron M, Tiraby G (1990) Cassettes of the *Streptoalloteichus hindustanus ble* gene for transformation of lower and higher eukaryotes to phleomycin resistance. *Nucleic Acids Res* 18:4009.
15. Sugino A, Peebles CL, Kreuzer KN, Cozzarelli NR (1977) Mechanism of action of nalidixic acid: Purification of *Escherichia coli nalA* gene product and its relationship to DNA gyrase and a novel nicking-closing enzyme. *Proc Natl Acad Sci USA* 74:4767–4771.
16. Cáceres NE, et al. (1997) Overexpression of the D-alanine racemase gene confers resistance to D-cycloserine in *Mycobacterium smegmatis*. *J Bacteriol* 179:5046–5055.
17. Banerjee A, et al. (1994) *inhA*, a gene encoding a target for isoniazid and ethionamide in *Mycobacterium tuberculosis*. *Science* 263:227–230.
18. Kremer L, et al. (2000) Thiolactomycin and related analogues as novel anti-mycobacterial agents targeting KasA and KasB condensing enzymes in *Mycobacterium tuberculosis*. *J Biol Chem* 275:16857–16864.
19. van Kessel JC, Hatfull GF (2007) Recombineering in *Mycobacterium tuberculosis*. *Nat Methods* 4:147–152.
20. Wilson M, et al. (1999) Exploring drug-induced alterations in gene expression in *Mycobacterium tuberculosis* by microarray hybridization. *Proc Natl Acad Sci USA* 96: 12833–12838.
21. Singh R, et al. (2008) PA-824 kills nonreplicating *Mycobacterium tuberculosis* by intracellular NO release. *Science* 322:1392–1395.
22. van Stelten J, Silva F, Belin D, Silhavy TJ (2009) Effects of antibiotics and a proto-oncogene homolog on destruction of protein translocator SecY. *Science* 325:753–756.
23. Kohanski MA, Dwyer DJ, Hayete B, Lawrence CA, Collins JJ (2007) A common mechanism of cellular death induced by bactericidal antibiotics. *Cell* 130:797–810.
24. Kohanski MA, Dwyer DJ, Wierzbowski J, Cottarel G, Collins JJ (2008) Mistranslation of membrane proteins and two-component system activation trigger antibiotic-mediated cell death. *Cell* 135:679–690.
25. Dwyer DJ, Kohanski MA, Hayete B, Collins JJ (2007) Gyrase inhibitors induce an oxidative damage cellular death pathway in *Escherichia coli*. *Mol Syst Biol* 3:91.
26. Kwon YK, Higgins MB, Rabinowitz JD (2010) Antifolate-induced depletion of intracellular glycine and purines inhibits thymineless death in *E. coli*. *ACS Chem Biol* 5: 787–795.
27. Argyrou A, Vetting MW, Aladegbami B, Blanchard JS (2006) *Mycobacterium tuberculosis* dihydrofolate reductase is a target for isoniazid. *Nat Struct Mol Biol* 13: 408–413.
28. Timmins GS, Master S, Rusnak F, Deretic V (2004) Requirements for nitric oxide generation from isoniazid activation in vitro and inhibition of mycobacterial respiration *in vivo*. *J Bacteriol* 186:5427–5431.
29. Slayden RA, Lee RE, Barry CE, 3rd (2000) Isoniazid affects multiple components of the type II fatty acid synthase system of *Mycobacterium tuberculosis*. *Mol Microbiol* 38: 514–525.
30. Drlica K (1999) Mechanism of fluoroquinolone action. *Curr Opin Microbiol* 2:504–508.
31. Hatfull GF, Jacobs WR, Jr. (2000) *Molecular Genetics of Mycobacteria* (ASM Press, Washington).
32. Franzblau SG, et al. (1998) Rapid, low-technology MIC determination with clinical *Mycobacterium tuberculosis* isolates by using the microplate Alamar Blue assay. *J Clin Microbiol* 36:362–366.
33. Siegrist MS, et al. (2009) Mycobacterial Esx-3 is required for mycobactin-mediated iron acquisition. *Proc Natl Acad Sci USA* 106:18792–18797.
34. Esaki N, Walsh CT (1986) Biosynthetic alanine racemase of *Salmonella typhimurium*: Purification and characterization of the enzyme encoded by the *alr* gene. *Biochemistry* 25:3261–3267.
35. de Carvalho LP, et al. (2010) Metabolomics of *Mycobacterium tuberculosis* reveals compartmentalized co-catabolism of carbon substrates. *Chem Biol* 17:1122–1131.